No tension between pulsar timing array upper limits on the nano-Hertz gravitational wave background and assembly models of massive black hole binaries

Hannah Middleton, Siyuan Chen, Walter del Pozzo, Alberto Sesana, Alberto Vecchio

No tension between pulsar timing array upper limits on the nano-Hertz gravitational wave background and assembly models of massive black hole binaries

No tension between pulsar timing array upper limits on the nano-Hertz gravitational wave background and assembly models of massive black hole binaries

Hannah Middleton[1,2], Siyuan Chen[1,3], Walter Del Pozzo[1,4], Alberto Sesana[1,5] and Alberto Vecchio[1]

[1] Institute of Gravitational Wave Astronomy and School of Physics and Astronomy, University of Birmingham, Birmingham B15 2TT, UK
[2] School of Physics, University of Melbourne, Parkville, Vic 3010, Australia and OzGrav Australian Research Council Centre of Excellence for Gravitational Wave Discovery
[3] Station de Radioastronomie de Nançay, Observatoire de Paris, PSL University, CNRS, Université dOrléans, 18330 Nançay, France and FEMTO-ST Institut de recherche, Department of Time and Frequency, UBFC and CNRS, ENSMM, 25030 Besançon, France and Laboratoire de Physique et Chimie de lEnvironnement et de lEspace, LPC2E UMR7328, Université dOrléans, CNRS, 45071, Orléan, France
[4] Dipartimento di Fisica "Enrico Fermi", Università di Pisa and INFN sezione di Pisa, Pisa I-56127, Italy
[5] Dipartimento di Fisica "G. Occhialini", Universita' degli Studi di Milano-Bicocca, Piazza della Scienza 3, 20126 Milano, Italy

E-mail: `hannah.middleton@unimelb.edu.au`

Abstract. Pulsar timing arrays provide a means to observe the nano-Hertz gravitational wave background from the population of merging massive black hole binaries. Observations are placing increasingly stringent upper limits on the gravitational wave background. Upper limits and future detections will enable the study of the properties of the merging population. Recent upper limits have cast doubt on current predictions of the gravitational wave background. Here we perform a Bayesian analysis comparing upper limits to astrophysical prediction. So far models are consistent with observation. These proceedings summarise previous work in Ref. [1].

1. Introduction

Hierarchical formation scenarios point towards frequent mergers of galaxies throughout cosmic time. It is likely that the evolution of the central massive black holes (MBH) within merging galaxies goes hand-in-hand with galaxy evolution, producing a population of merging MBH binaries (MBHBs). To date, there are several MBHB candidates (e.g. [2, 3]), however confirming these observations remains challenging [4]. Gravitational wave (GW) searches at nano-Hertz (nHz) frequencies will provide insight into the properties of this population. Many merging binaries produce a stochastic GW background (GWB). Timing a selection of ultra-stable millisecond pulsars creates a galactic-scale GW detector [5]. Pulsar timing array (PTA) campaigns around the world are hunting for the nHz GWB. No detection has been made so far, however the three PTA consortia have been progressively placing more constraining upper limits on the GWB (however recent work on the effect of solar system ephemeris errors show there

is some upward revision of the upper limit [6]). The PTAs are: the Parkes PTA (PPTA [7]); the European PTA (EPTA [8]); and the North American Nanohertz Observatory for Gravitational Waves (NANOGrav [6]). Together they form the International PTA (IPTA [9]).

Here we consider the implication of PTA upper limits on the properties of the merging MBHB population. The most constraining upper limit on the characteristic strain of the GWB is from the PPTA, with a 95% confidence upper limit of 1×10^{-15} at a GW frequency of $f = 1\,\mathrm{yr}^{-1}$ [10]. It has been suggested that this upper limit is in tension with the current understanding of MBHB formation scenarios. Here we use a Bayesian analysis with a generic model of the MBHB population to compare the upper limit with astrophysical prediction. We find the upper limit to be consistent so far.

In section 2, we briefly overview the model for the population of MBHBs, and in section 3 we describe the astrophysical priors for our Bayesian analysis. Our results and conclusions are summarised in sections 4 and 5 respectively. For detailed information on this work, see Ref. [1], on which these proceedings are based.

2. Model of the population

The GW background is determined by the merger rate and the MBHB population properties. A population of circular binaries evolving via radiation reaction alone results in a GW spectrum with characteristic strain $h_\mathrm{c}(f) \propto f^{-2/3}$ [11]. However, the process from galaxy merger to efficient GW emission requires the binary to tighten to a separation where GW emission is the dominant factor in the binary evolution. To reach this point, the binary may exchange energy and angular momentum with the stellar and/or gaseous environment, possibly resulting in a non-zero eccentricity. Eccentricity modifies the $f^{-2/3}$ spectrum, leading to a depletion of sources at low frequencies where PTAs are most sensitive. Full details of the description of the spectrum are in Ref. [12]. Here we briefly summarise the model and its parameters.

The binary evolution transitions from environmental driven to GW driven at frequency f_t with eccentricity e_t and proceeds to circularise via GW emission. The GW spectrum for a given binary is determined by the chirp mass $\mathcal{M} = (M_1 M_2)^{3/5}/(M_1 + M_2)^{1/5}$ (where M_1 and M_2 are the component masses), redshift z, f_t and e_t. The GWB is set by the total contribution from the population of MBHB,

$$h_\mathrm{c}^2(f) = \int \mathrm{d}z \int \mathrm{d}\log_{10}\mathcal{M} \frac{\mathrm{d}^2 n}{\mathrm{d}\log_{10}\mathcal{M}\mathrm{d}z} h_\mathrm{c,fit}^2 \left(f\frac{f_\mathrm{p,0}}{f_\mathrm{p,t}}\right) \left(\frac{f_\mathrm{p,t}}{f_\mathrm{p,0}}\right)^{-4/3} \left(\frac{\mathcal{M}}{\mathcal{M}_0}\right)^{5/3} \left(\frac{1+z}{1+z_0}\right)^{-1/3}, \quad (1)$$

where $h_\mathrm{c,fit}$ is an analytic fit to the GW spectrum of a reference binary with $\mathcal{M} = \mathcal{M}_0$, $z = z_0$, and eccentricity e_0 at reference frequency f_0. The reference values are computed at the peak frequency of the spectrum $f_\mathrm{p,0}$ and the actual contribution of a binary with a given $\mathcal{M}$, z, e_t and f_t is found by rescaling the spectrum to the required turn over peak $f_\mathrm{p,t}$ ($f(f_\mathrm{p,0}/f_\mathrm{p,t})$) [12]. The distribution of binaries in equation 1 is given by

$$\frac{\mathrm{d}^2 n}{\mathrm{d}\log_{10}\mathcal{M}\mathrm{d}z} = \dot{n}_0 \left(\frac{\mathcal{M}}{10^7 \mathrm{M}_\odot}\right)^{-\alpha} \exp\left(-\frac{\mathcal{M}}{\mathcal{M}_*}\right) (1+z)^\beta \exp\left(-\frac{z}{z_*}\right) \frac{\mathrm{d}t_\mathrm{r}}{\mathrm{d}z}, \quad (2)$$

where $\mathrm{d}t_\mathrm{r}/\mathrm{d}z$ is the time-redshift relation assuming a standard ΛCDM and cosmological constant $H_0 = 70\,\mathrm{km\,s^{-1}\,Mpc^{-1}}$. Equation 2 has five free parameters: $\dot{n}_0$ is the co-moving number of mergers per Mpc^3 per Gyr; the slope and cut-off of the $\mathcal{M}$ distribution are controlled by α and $\mathcal{M}_*$ respectively; and similarly the shape of the z distribution is set by β and z_*. The eccentricity parameter described above, plus these five uniquely describe the GW spectrum, resulting in six parameters in total $\theta = \{\dot{n}_0, \beta, z_*, \alpha, \mathcal{M}_*, e_\mathrm{t}\}$.

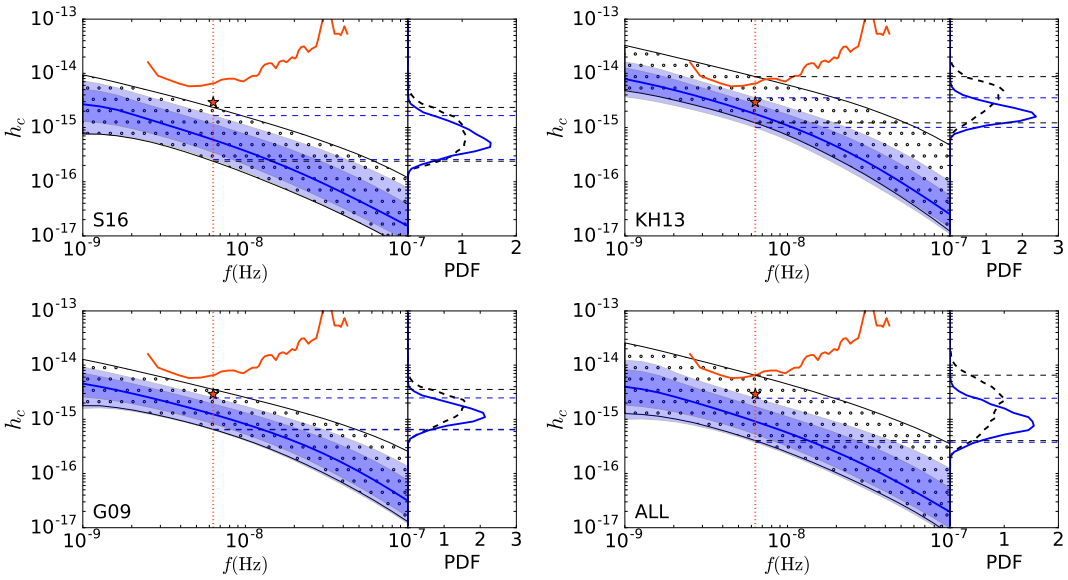

Figure 1. Comparing the prior and posterior distributions given the PPTA upper limit. The four panels show the results for each of the astrophysical predictions (S16 top-right; KH13 top-left; G09 bottom-right; ALL bottom-left). The posterior distribution of $h_c(f)$ is shown by the blue-shaded banding (light and dark for the 68% and 90% confidence bands respectively and the solid-blue line shows the median). The 90% confidence band of the prior probability distribution is shown by the black-dotted region. For comparison, the orange curve shows the PPTA frequency-dependent upper limit, with the integrated upper limit for $h_c(f) \propto f^{-2/3}$ indicated by the orange star and vertical line. The right-hand plots of each panel show a cross-section of the prior (black-dash) and posterior (blue-solid) at $f \sim 1/5\mathrm{yr}^{-1}$ with the central 90% regions marked by black- and blue- dashed lines respectively). Reproduced from our main publication [1].

3. Astrophysical Prior and Bayesian analysis

Our goal is to compare the most stringent PTA upper limit with current astrophysical predictions. We consider a set of models whose predicted GWB spans a range of levels with the use of different MBH–host galaxy scaling relations (for full details of the models see Refs. [13, 14, 1]). Each model can be summarised by the median GW strain it predicts at $f = 1\,\mathrm{yr}^{-1}$. They are: (i) an optimistic prediction of 1.5×10^{-15} labelled KH13 [15]; (ii) a moderate prediction of 7×10^{-16} labelled G09 [16]; (iii) a conservative prediction of 4×10^{-16} we label S16 [17]; and (iv) a combination of the other models plus others, spanning a range of two orders of magnitude with a median value of 8×10^{-16} which we label ALL. These astrophysical predictions inform the prior of our model parameters in section 2.

Using Bayesian analysis, we compute the posterior probability distribution on the model parameters given the PTA data and our model as described above (see also Refs. [18, 19, 20]). We use a nested sampling algorithm [21] to compute the posterior distributions.

4. Results

Our main results are summarised by figure 1. It is useful to convert the posterior distribution for the six parameters into a posterior distribution on the GW spectrum $h_c(f)$ as shown. The dotted region is the prior informed by the astrophysical predictions and the shaded blue bands are the posterior. For comparison, the orange line shows the 95% confidence upper limit on the

GW background from the PPTA [10]. The one-dimensional distributions show a cross-section of the posterior and prior. Each panel shows one of the astrophysical predictions described in section 3 (labelled in the bottom-left of each panel). The degree of consistency between each model can be judged by the difference between the prior and posterior. We see that in all cases, the top of the prior distribution is removed by the upper limit, however all astrophysical predictions remain consistent with the upper limit.

5. Conclusions

Upper limits are beginning to reach sensitivities where meaningful comparisons can be made with astrophysical predictions of the MBHB population. At this stage, we find that current upper limits are fully consistent with prediction. Standard formation scenarios do not require additional physics to explain the lack of detection, i.e. eccentricity, accelerated mergers via strong interaction with the environment or stalled/inefficient MBHB formation. Recent work to more closely relate the population model with astrophysical observables also supports this conclusion [18]. On the other hand, we see that PTA observations are beginning to provide interesting information on the MBHB population (for example KH13 is disfavoured against the more conservative S16). As PTA sensitivities improve, future upper limits and detections will be informative for our understanding of the MBHB population.

Acknowledgments

HM and AV acknowledge support from the Science and Technology Facilities Council (STFC). SC acknowledges the support of the University of Birmingham via the AE Hills scholarship. AS acknowledges support by a URF of the Royal Society. HM also acknowledges support from Australian Research Council Centre of Excellence for Gravitational Wave Discovery (OzGrav) (project number CE170100004).

References

[1] Middleton H, Chen S, Del Pozzo W, Sesana A and Vecchio A, 2019, *Nature Communications* **9** 573
[2] Graham M J, Djorgovski S G, Stern D, Drake A J, Mahabal A A, Donalek C, Glikman E, Larson S and Christensen E, 2015, *MNRAS* **453** 1562–76
[3] Krause M G H, Shabala S S, Hardcastle M J, Bicknell G V, Böhringer H, Chon G, Nawaz M A, Sarzi M and Wagner A Y, 2019, *MNRAS* **482** 240–61
[4] Vaughan S, Uttley P, Markowitz A G, Huppenkothen D, Middleton M J, Alston W N, Scargle J D and Farr W M, 2016, *MNRAS* **461** 3145–52
[5] Foster R S and Backer D C, 1990, *Ap J* **361** 300–8
[6] Arzoumanian Z *et al*, 2018, *Astrophysical Journal, Supplement* **235** 37
[7] Reardon D J *et al*, 2016, *MNRAS* **455** 1751–69
[8] Desvignes G *et al*, 2016, *MNRAS* **458** 3341–80
[9] Verbiest J P W *et al*, 2016, *MNRAS* **458** 1267–88
[10] Shannon R M *et al.* 2015, *Science* **349** 1522–5
[11] Phinney E S, 2001, *arXiv e-prints* astro-ph/0108028
[12] Chen S, Sesana A and Del Pozzo W, 2017, *MNRAS* **470** 1738–49
[13] Sesana A, 2013, *MNRAS* **433** L1–5
[14] Sesana A, Shankar F, Bernardi M and Sheth R K, 2016, *MNRAS* **463** L6–11
[15] Kormendy J and Ho L C, 2013, *ARA&A* **51** 511–653
[16] Gültekin K *et al*, 2009, *Astrophys. J.* **698** 198–221
[17] Shankar F, Bernardi M, Sheth R K, Ferrarese L, Graham A W, Savorgnan G, Allevato V, Marconi A, Läsker R and Lapi A, 2016, *MNRAS* **460** 3119–42
[18] Chen S, Sesana A and Conselice C J, 2019, *MNRAS* **488** 401–18
[19] Chen S, Middleton H, Sesana A, Del Pozzo W and Vecchio A, 2017, *MNRAS* **468** 404–17
[20] Middleton H, Del Pozzo W, Farr W, Sesana A and Vecchio A, 2016, *MNRAS* **455** L72–6
[21] Veitch J, Del Pozzo W, Cody, Pitkin M and ed1d1a8d, 2017, johnveitch/cpnest: Minor optimisation (Version 0.1.4), *Zenodo* http://doi.org/10.5281/zenodo.835874